^{55}Mn NMR investigation of $Nd_{1-x}Sr_xMnO_3$ ($0.1 \leqslant x \leqslant 0.5$)

M. Pattabiraman, P. Murugaraj,* and G. Rangarajan†
Department of Physics, Indian Institute of Technology, Madras, Chennai-600 036, India

C. Dimitropoulos and J-Ph. Ansermet
Institut de Physique Experimentale, EPFL-PH-Ecublens, 1015 Lausanne, Switzerland

G. Papavassiliou
Institute of Materials Science, National Centre for Scientific Research, "Demokritos," 15310 Athens, Greece

G. Balakrishnan, D. McK. Paul, and M. R. Lees
Department of Physics, University of Warwick, Coventry CV4 7AL, United Kingdom
(Received 29 January 2002; revised manuscript received 16 July 2002; published 18 December 2002)

^{55}Mn nuclear magnetic resonance (NMR) in $Nd_{1-x}Sr_xMnO_3$ ($0.1 \leqslant x \leqslant 0.5$) manganites provides local evidence of the magnetic inhomogeneities arising from the electronic structure changes below T_C. The temperature dependences of magnetization, resistivity, and NMR spectra were compared in samples in the ferromagnetic insulating, ferromagnetic metallic, and charge-ordered phases. Spin-spin relaxation enhancement around 15 K is attributed to a critical slowing down of the Nd sublattice.

DOI: 10.1103/PhysRevB.66.224415 PACS number(s): 76.60.Lz, 71.30.+h

I. INTRODUCTION

It has now been well established that the physics of manganites exhibiting colossal magnetoresistance (CMR) is governed by an interplay of the double exchange interaction, electron-phonon coupling via the Jahn-Teller interaction, and the ionic size effect resulting in a complex phase diagram.[1] The strong electron-phonon coupling results in polaron formation and determines the mobility of the charge carriers and hence the strength of the double exchange interaction. Over the last few years, various theoretical and experimental studies have shown that the manganites are susceptible to a ''phase separation'' into carrier-rich and carrier-poor regions. This is believed to be the source of CMR, since the carrier-rich regions grow upon application of a magnetic field resulting in a large negative MR.[2–5] Nuclear magnetic resonance (NMR), a direct probe of the microscopic magnetization in a solid, has been used to detect this ''phase separation'' in $La_{1-x}Ca_xMnO_3$ (LCMO).[6,7] In this paper we present ^{55}Mn spin-echo NMR amplitude and relaxation time measurements on the $Nd_{1-x}Sr_xMnO_3$ [NSMO(x)] family. The ferromagnetic metals in the NSMO family exhibit many interesting properties. For example, in thin films of $Nd_{0.7}Sr_{0.3}MnO_3$ CMR values ($-\Delta R/R_H$) as large as 10^6% at 60 K and 8 T (four orders change in resistance)[8]—the largest ever reported—and 5×10^4% in bulk samples[9] have been observed. Magnetization and dynamical studies of the time-dependent magnetization of $Nd_{0.7}Sr_{0.3}MnO_3$ have shown the presence of inhomogeneous magnetic order and spin frustration below T_C.[10] Neutron-scattering measurements show that the spin correlation length remains small $\sim$20 Å and nearly temperature independent around T_C and grows to 100 Å at about $0.95T_C$ unlike in a conventional ferromagnet.[11] Recent Raman scattering and optical measurements on $Nd_{0.7}Sr_{0.3}MnO_3$ point to the existence of dynamic Jahn-Teller interactions.[12,13] All these measurements have led to speculation about the nature of the inhomogeneous magnetism that is observed just below T_C. We used ^{55}Mn NMR as a local probe and provide clear evidence of inhomogeneous magnetism in doped NSMO manganites just below T_C. Also of interest in the $Nd_{1-x}Sr_xMnO_3$ system is the possibility of a strong Nd-Mn interaction. Neutron-scattering measurements in $Nd_{0.7}Sr_{0.3}MnO_3$ (Ref. 14) show that the Nd spins order below 20 K, leading to the canting of the Mn spins at lower temperatures. New spin-wave modes have been detected in $Nd_{0.6}Sr_{0.4}MnO_3$ at 11 K, which are attributed to a strong Nd-Mn exchange.[15] The Nd-spin ordering transition is manifested as a low-temperature minimum in the temperature dependence of the ^{55}Mn spin-spin relaxation time (T_2).

II. EXPERIMENT

Polycrystalline $Nd_{1-x}Sr_xMnO_3$ ($x=0.1,0.3,0.4$) samples were prepared by the standard solid-state reaction method. Stoichiometric amounts of Nd_2O_3, $SrCO_3$, and MnO_2 were wet mixed and the resulting slurry was calcined at 1200 °C for 24 h. This procedure was repeated thrice with intermediate grindings to ensure better homogeneity. For transport studies the powder was pelletized and sintered at 1500 °C for 4 h. Single crystals of NSMO ($x=0.5$) grown in an infrared image furnace by the floating zone technique were also used in the present investigation. Details about the crystal growth technique can be found elsewhere.[16] The samples were characterized by x-ray diffraction, resistivity, and magnetization measurements. Electrical resistivity measurements were performed using the standard four-probe method and magnetization data were obtained using a MPMS quantum design superconducting quantum interference device magnetometer and a commercial ac susceptometer (SCR-204T, Sumitomo Heavy Industries Ltd., Japan). The ^{55}Mn NMR spin-echo amplitude and relaxation time measurements were performed

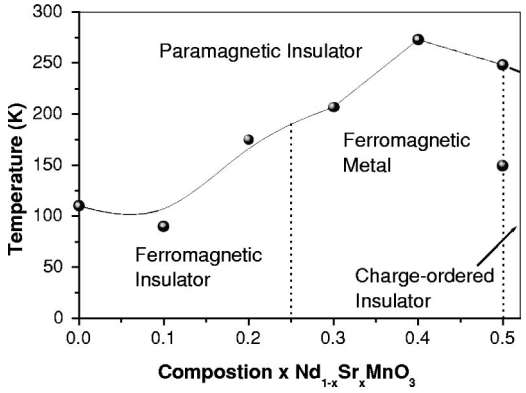

FIG. 1. Phase diagram for $Nd_{1-x}Sr_xMnO_3$ based on magnetization and resistivity measurements by Yoshizawa *et al.* (Ref. 18).

with an untuned probe head with a 1 μsec–τ–2 μsec spin-echo pulse sequence with $\tau=2$ μsec using a home-built spectrometer. The spin-lattice relaxation time (T_1) was measured using the saturation-recovery technique. The spin-spin relaxation time (T_2) was obtained by measuring the echo amplitude as a function of the delay between the two pulses. The application of NMR techniques to ferromagnetic materials allows the study of the local magnetic states via the hyperfine interactions, as probed by the resonant response of nuclear magnetic moments at individual atomic sites. Resonance occurs at a frequency ν given by $2\pi\nu=\gamma B_e=A\langle S\rangle/\hbar$, where γ is the nuclear gyromagnetic ratio ($\gamma/2\pi=10.553$ MHz T^{-1} for ^{55}Mn), B_e is the effective internal magnetic field, arising mainly from hyperfine interactions, A is the hyperfine coupling constant, and $\langle S\rangle$ the average Mn spin. Since $\langle S\rangle$ for a Mn^{3+} ion is 2 and 3/2 for a Mn^{4+} ion, ^{55}Mn NMR can distinguish between different Mn charge states. In ferromagnetic solids the applied rf field tilts the electronic magnetization (and hence the hyperfine field) from its equilibrium position giving rise to a transverse component of B_e. Since $B_e \gg B_{rf}$, the effective field experienced by the nuclei is much higher than that actually applied. This ''rf enhancement'' is a typical feature of NMR in ferromagnetic solids.[17]

III. RESULTS

A. Resistivity and magnetization measurements

The existing phase diagram for the NSMO system[18] (Fig. 1) indicates that the compounds with $0<x<0.25$ are ferromagnetic insulators (FMI) and compounds with $0.25<x<0.5$ are ferromagnetic metals (FMM). NSMO ($x=0.5$) exhibits charge ordering below the ferromagnetic transition. Our magnetic and transport measurements of samples with $x=0.1$, $x=0.3$–0.4, and $x=0.5$ are in agreement with the above classification.

The temperature dependences of the resistivity [$\rho(T)$] and the magnetization [$M(T)$] in an applied field of 1 T for NSMO (0.1) are shown in Figs. 2(a, b). The $M(T)$ data up to 127 K [Fig. 2(a)] could be fitted to an equation of the form $M=M_o(1\text{-}T/T_C)^{\beta}$ with $T_C=144$ K and $\beta=0.35$.

The nonlinear behvior of the M-H plot [Figs. 3(a, b)] is a

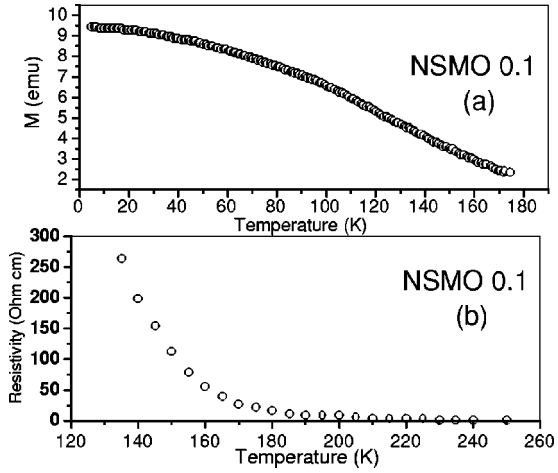

FIG. 2. Temperature dependences of magnetization in a field of 1 T (a) and resistivity at zero field (b) for NSMO 0.1.

clear indication of the presence of ferromagnetic exchange. The hysteresis collapses at temperatures higher than 5 K, suggestive of a superparamagnetic behavior of localized regions.[19]

The simultaneous transition from a paramagnetic insulator to a ferromagnetic metal is shown for NSMO 0.3 (polycrystalline), and NSMO 0.4 in Figs. 4(a, b). The decrease in magnetization in the ZFC route for both compositions is due to canting of Mn spins and is discussed further below.

NSMO 0.5 exhibits a transition from a paramagnetic insulator to a ferromagnetic metal around 248 K. Upon further cooling there is an ordering of the Mn^{3+} and Mn^{4+} ions in the lattice.[20] This is accompanied by a ferromagnetic-antiferromagnetic transition around 148 K (T_{CO}); cooling route that is seen in the temperature dependence of the real part of the ac susceptibility (χ') [Fig. 5(a)] and strong carrier localization as seen by the sudden rise in resistance [Fig. 5(b)]. A jump in the lattice constants was also reported at

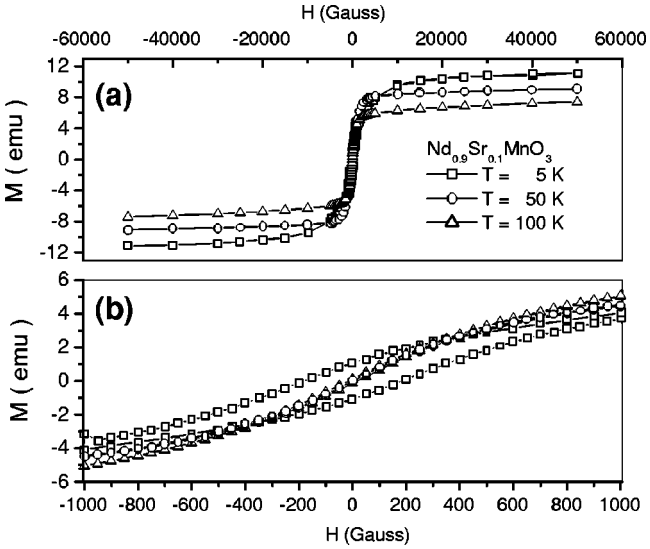

FIG. 3. Hysteresis loops for NSMO 0.1 (a). The low field response is shown in (b).

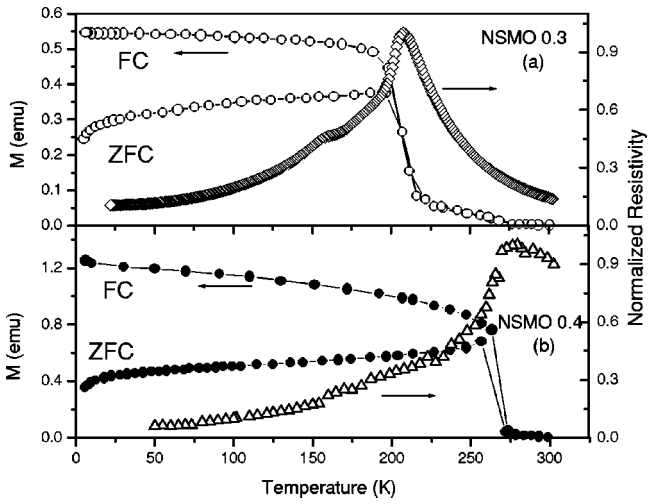

FIG. 4. Temperature dependence of magnetization and resistivity for polycrystalline NSMO 0.3 (a) and NSMO 0.4 (b). The resistivity values are normalized with respect to the value observed at the resistivity peak. The magnetization measurements were performed in an applied field of 100 G. T_p is the metal-insulator transition temperature.

T_{CO}.[21] The hysteresis observed in $\rho(T)$ and $M(T)$ across the charge-ordering (CO) transition temperature (T_{CO}) is indicative of a first-order transition.

B. ^{55}Mn NMR measurements

The spin-echo amplitude as a function of frequency for NSMO ($0.1 \leqslant x \leqslant 0.4$) at 6 K is shown in Figs. 6(a, b, c). The prominent peak that is observed at 427 MHz in NSMO 0.1 [Fig. 6(a)] is attributed to a charge state of Mn^{3+} and the peak at 325 MHz is attributed to a charge state of Mn^{4+}.[22] This assignment is based on the estimates of the hyperfine fields for Mn^{4+} and Mn^{3+} by Freeman and Watson[23] and is further substantiated by hyperfine field data obtained from

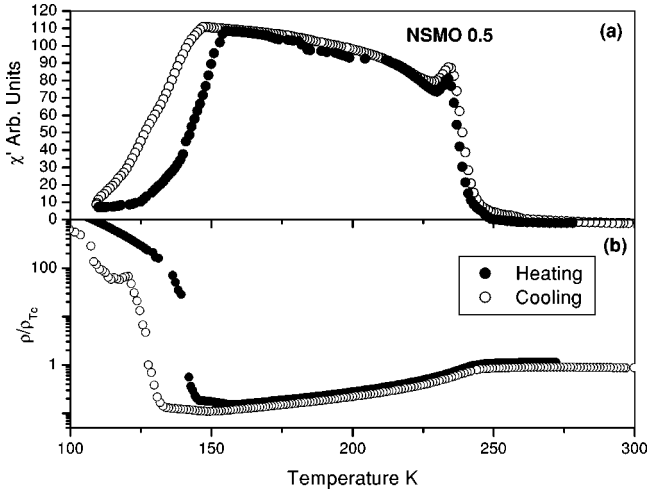

FIG. 5. Temperature dependence of magnetization (a) and resistivity (b) for NSMO 0.5. T_{CO} is the charge-ordering temperature. The resistivity values are normalized with respect to the value observed at the resistivity peak.

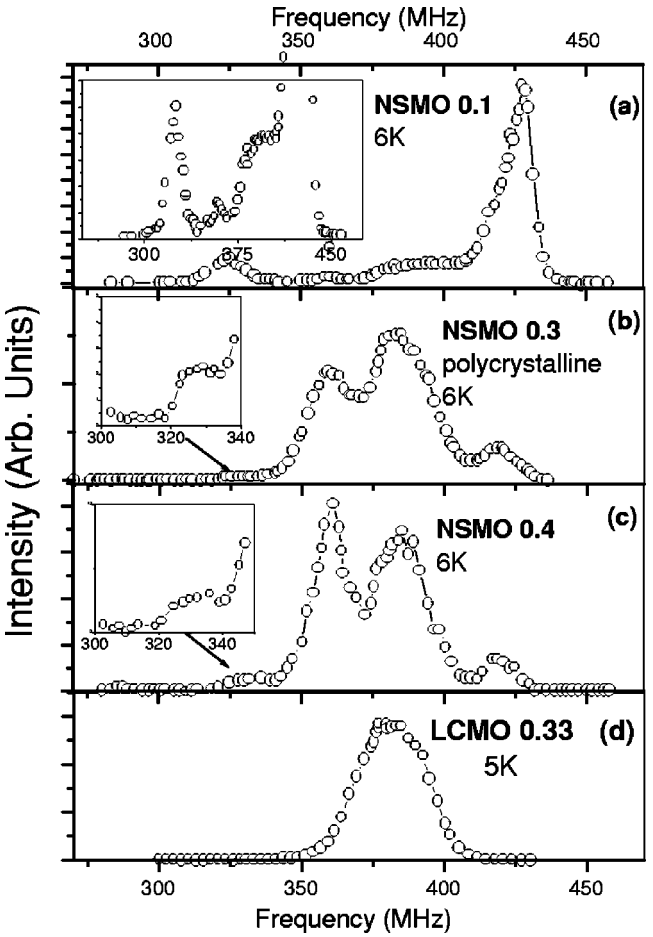

FIG. 6. (a), (b), (c) Spin-echo amplitude for NSMO (0.1, 0.3, 0.4, respectively). The insets show the low-amplitude features of the spectrum. (d) The spin-echo spectrum for $La_{0.67}Ca_{0.33}MnO_3$ (LCMO 0.33) at 5 K is also plotted for comparison.

NMR studies on $MnFe_2O_4$ (Mn^{3+}) (Ref. 24) and $LiMn_{3.5}Fe_{1.5}O_8$ (Mn^{4+}).[25] Above 6 K, the spin-echo amplitude diminished rapidly, becoming undetectable for NSMO 0.1.

For the ferromagnetic metals, NSMO 0.3 and 0.4, a prominent double-peak structure is observed between 340 MHz and 400 MHz. In most ferromagnetic manganites in which ^{55}Mn NMR has been studied,(e.g., $La_{0.7}Ca_{0.3}MnO_3$, $La_{0.69}Ca_{0.31}MnO_3$) (Refs. 22,26) a single broad peak is observed between the Mn^{3+} and Mn^{4+} resonances. For reasons of comparison we have plotted in Fig. 6(d) a typical spectrum of $La_{0.67}Ca_{0.33}MnO_3$ at 5 K, which is ferromagnetic and metallic. A single broad peak around 382 MHz is observed between the Mn^{3+} and Mn^{4+} resonances. The peak frequency of the signal at intermediate frequencies was found to scale with the average Mn spin state ($\langle S \rangle$).[26] Moreover, the signal intensity increases with increase in alkaline-earth doping and (hence) decrease in resistivity.[22] Therefore, the intermediate signal is likely to arise from the fast hopping of carriers from Mn^{3+} and Mn^{4+} resulting in a hyperfine field corresponding to an averaged Mn^{3+}/Mn^{4+} state due to the double exchange interaction (DEX), which is proportional to the amount of alkaline earth in the sample. However, in case

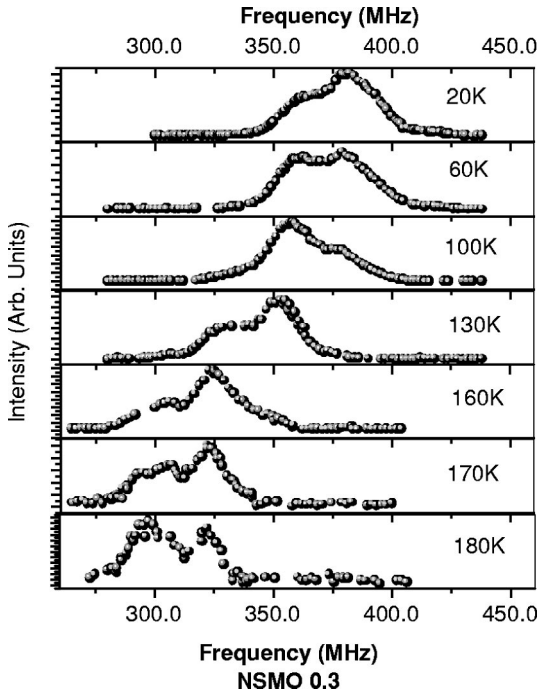

FIG. 7. Temperature dependence of the spin-echo amplitude for NSMO 0.3 ($T_C = 207$ K).

of NSMO 0.3 and 0.4, a double-peaked DEX signal is observed, instead of a single-peaked one, the origin of which will be discussed below.

The temperature dependence of the spin-echo amplitude (Boltzmann corrected—multiplied with T) for both compositions is plotted in Figs. 7 and 8.

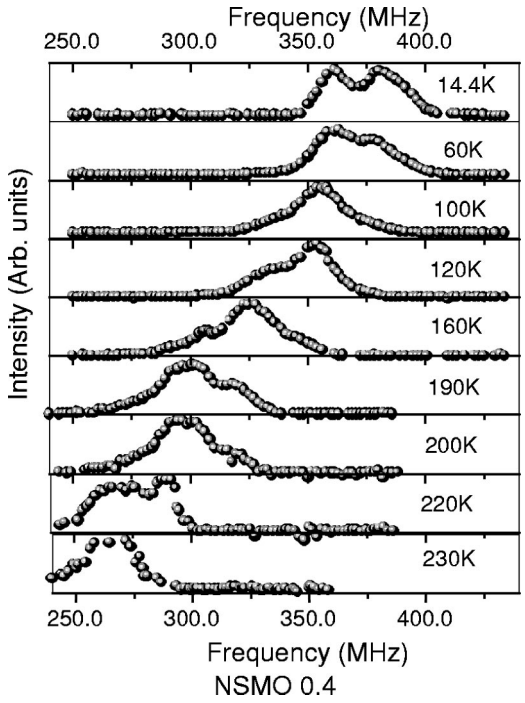

FIG. 8. Temperature dependence of the spin-echo amplitude for NSMO 0.4($T_C = 273$ K).

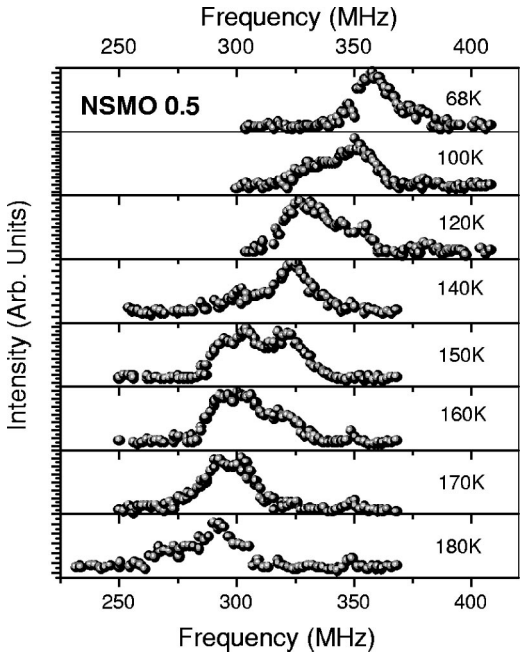

FIG. 9. Temperature dependence of the spin-echo amplitude for NSMO 0.5 ($T_C = 234$ K, $T_{CO} = 148$ K).

Upon heating, the high-frequency component of the DEX signal progressively dies out and so does the Mn^{3+} signal. With further increase in temperature, tails appear around 330 MHz and 310 MHz above 110 K and 140 K, respectively, for NSMO 0.3 which develop into peaks upon heating. The evolution of the spin-echo spectrum for NSMO 0.4 also follows a similar trend. The NMR spin-echo amplitude for NSMO 0.5 as a function of temperature is shown in Fig 9. Since the system becomes a charge-ordered antiferromagnetic insulator below 150 K, it was not possible to obtain the spin-echo signal below 60 K for the rf power levels used. In contrast to $\rho(T)$ and $M(T)$ data [Figs. 5(a, b)] and previous ^{55}Mn reports on LCMO 0.5 (Ref. 27) we do not find any thermal hysteresis across T_{CO} in the spectra.

The peak frequencies observed in the spin-echo spectrum for NSMO 0.3, 0.4, and 0.5 when plotted together (Fig. 10) suggests that upon heating the DEX signal disappears above 150 K for NSMO 0.3 and 160 K for NSMO 0.4. Although the transport properties $[\rho(T)]$ of NSMO 0.5 are quite different from those of NSMO 0.3 and NSMO 0.4, it has a similar temperature dependence of its ^{55}Mn-NMR spectrum. Instead of a progressive change of frequency with temperature, we observe the appearance and coexistence of peaks. This is quite different from the result in LCMO, in which the Mn double peak shifts progressively as the temperature is lowered from T_C to 0 K. This weak temperature dependence was noticed in other manganates.[28]

Figures 11(a, b) show the temperature dependence of T_1 for NSMO 0.3 and 0.4. Below 50 K the values were too small to be measured accurately. Figures 12(a, b) show the temperature dependence of T_2 measured at the different peak frequencies for NSMO 0.3 and 0.4, respectively. It is seen that both T_1 and T_2 decrease below 90 K for both NSMO 0.3 and 0.4, unlike the behavior expected in a ferromagnet.

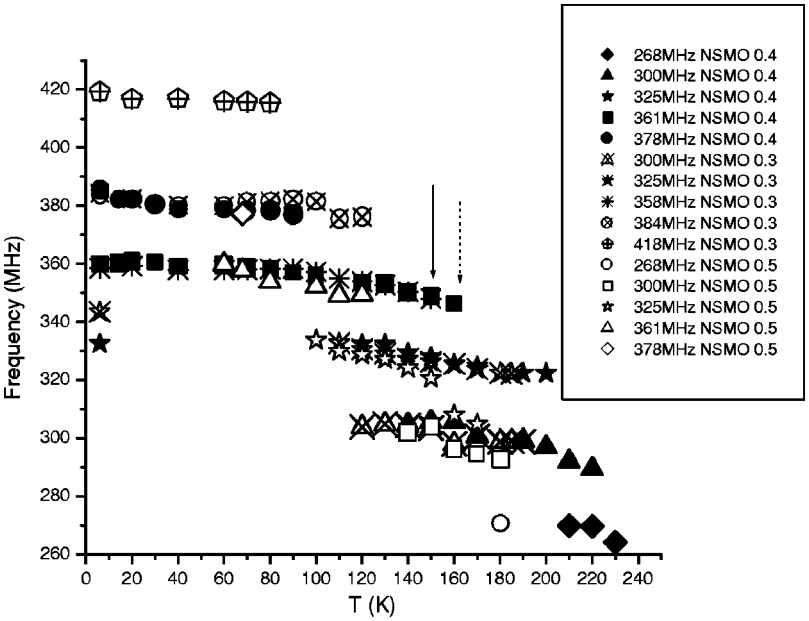

FIG. 10. Temperature dependence of the peak frequencies of the spin-echo spectrum for NSMO 0.3 (crossed symbols), NSMO 0.4 (filled symbols), and NSMO 0.5 (open symbols). The arrows mark the disappearance of the DEX signal upon heating for NSMO 0.3 (solid arrow) and NSMO 0.4 (dotted arrow).

IV. DISCUSSION

A. The spin-echo line shape and its temperature dependence for NSMO 0.3 and 0.4

In order to understand the temperature evolution of the spin-echo spectrum in NSMO 0.3 and 0.4, we consider two temperature ranges: (1) above 90 K, in which the low-frequency peaks that appear around 275–330 MHz are observed and (2) below 90 K, in which only the DEX signals are observed. We first consider the region above 90 K. The spectrum in this temperature range consists of two peaks around 358 MHz and 325 MHz upto 160 K for NSMO 0.3 and 120 K for NSMO 0.4. Above these temperatures additional peaks are observed at lower frequencies. The observation of a low-frequency signal in addition to the DEX signal upon heating a ferromagnetic metallic manganite has been reported before.[27,29] From a study of the ^{55}Mn spin-echo spectrum for $La_{1-x}Ca_xMnO_3$ as function of Ca composition, the low-frequency signal was interpreted as arising from a coexistence of FMM and FMI regions. Thus it is likely that the temperature region from 160 K to T_C is characterized by low carrier mobility due to a coexistence of FMM and FMI regions. This is in good agreement with recent synchrotron x-ray scattering studies on NSMO 0.3 (Ref. 30) which reveal the existence of charge/orbitally ordered (COO) regions (which promote carrier localization) below T_C.

The temperature dependence of the multipeaked spectrum can be characterized, in a first approximation, by the temperature dependence of its center of gravity (Fig. 13). We find a clear deviation from the mean-field prediction of the Heisenberg ferromagnet. The kink observed around $0.7T/T_C$ in the temperature dependence of the center of gravity corresponds to the disappearance of the DEX signal (Fig. 10) and coincides with a shoulder observed in the temperature dependence of the resistivity [Fig. 4(a)]. It is probable that the weak temperature dependence of the spin-spin correlation length just below T_C obtained from neutron-diffraction data[11] is also linked with such localization effects.

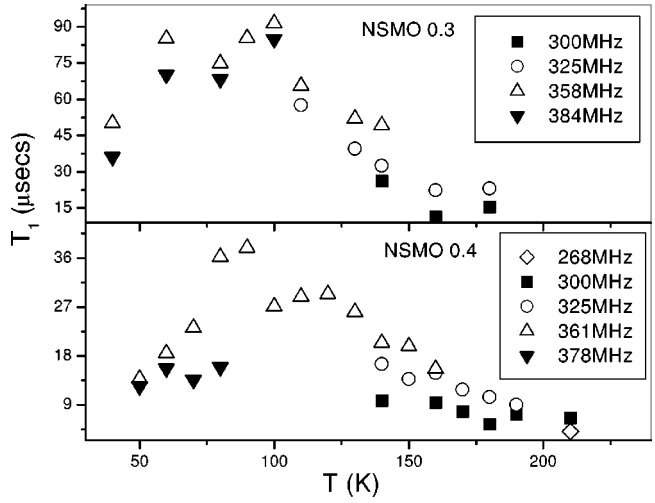

FIG. 11. Temperature dependence of T_1 for (a) NSMO 0.3 and (b) 0.4.

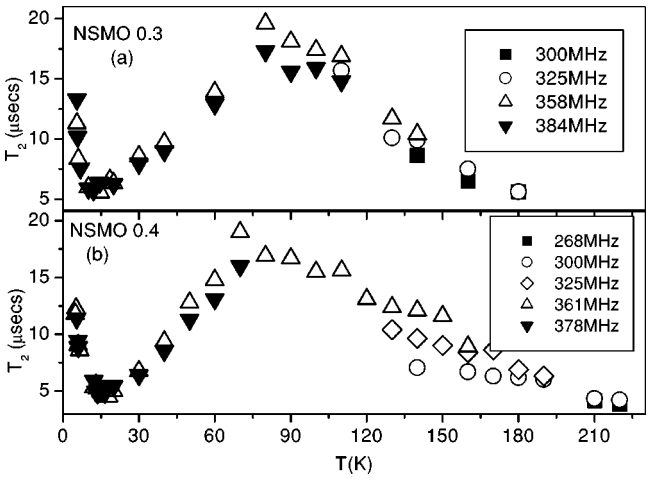

FIG. 12. Temperature dependence of T_2 for NSMO 0.3 (a) and NSMO 0.4 (b).

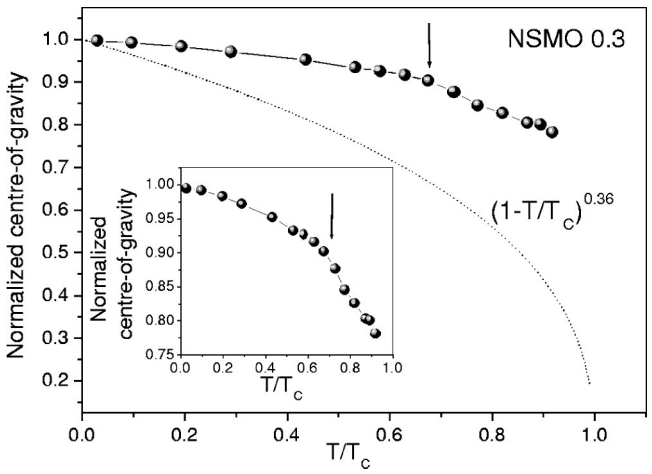

FIG. 13. Temperature dependence of the center of gravity (CoG) of the NMR spectrum for NSMO 0.3 compared with the typical temperature dependence of the order parameter of a Heisenberg ferromagnet (dotted line). The kink in the CoG is seen better in the inset and is marked by arrows.

Upon heating below T_C the abrupt shift of the spin-echo spectrum to higher frequencies in NSMO 0.3 and 0.4 coincides with the onset of anomalous softening of an envelope of two MnO_6 (around 450–482 cm^{-1}) bending modes, one of which is associated with the Jahn-Teller distortion.[12] It is plausible that the remarkable coincidence of these diverse quantities, taking into account the recent results of x-ray synchrotron measurements,[30] could arise from a disruption of the COO regions in the lattice below $0.7T/T_C$. The center of gravity kink (Fig. 13) coinciding with a shoulder observed in the temperature dependence of the resistivity of NSMO 0.3 (Fig. 4) is further supportive of such a scenario.

B. Influence of Nd-spin ordering on ^{55}Mn NMR

The temperature dependences of T_1 and T_2 (Figs. 11 and 12) point to an enhancement in the relaxation rate below 90 K, indicative of a critical slowing down of magnetic (hyperfine field) fluctuations at the position of the Mn nuclei below 90 K. A minimum of T_2 is found in NSMO 0.3 and NSMO 0.4 sample around 15 K. This T_2 minimum occurs in the temperature region where the zero-field-cooled magnetization exhibits a sudden dip [Figs. 4(a, b)] and where a Schottky-like specific heat anomaly in $Nd_{0.67}Sr_{0.33}MnO_3$ has been reported.[31] It is also the region in which neutron measurements reveal the ordering of Nd spins.[14] Hence it is likely that the T_2 minimum is associated with the ordering of Nd moments. The observation of a broad and shallow T_2 minimum suggests that Nd-spin ordering could occur through a gradual spin-freezing process. There is noticeable change in the spin-echo amplitude of NSMO 0.3 and NSMO 0.4 when heated to 20 K (Figs. 7 and 8) from 6 K [Figs. 6(b, c)]. The Mn^{4+} signal observed as a weak shoulder at 6 K is absent at 20 K. The Mn^{3+} peak observed at 6 K is seen only as a shoulder at 20 K. The DEX peaks appear less resolved at 20 K compared to 6 K. These changes are likely to be due to the canting of Mn spins (due to the strong Nd-Mn interaction) which has been observed by neutron diffraction and Mossbauer studies below the Nd-spin ordering temperature ($\sim$20 K).[14,32] The appearance of the Mn^{3+} and Mn^{4+} signal at 6 K [Figs. 6(b, c)] points to localization of a fraction of charge carriers due to the Mn-spin canting.

The double humped DEX peak may arise from the presence of two Mn-spin species that differ in the extent to which they couple with Nd spins resulting in two different hyperfine fields. However, other possible explanations for the double-peak DEX structure, such as variations in rf enhancement factor, cannot be ruled out.

C. The spin-echo line shape and its temperature dependence for NSMO 0.5

Based on a study of ^{139}La and ^{55}Mn NMR on $La_{0.5}Ca_{0.5}MnO_3$,[6,29] it has been reported that below T_{CO} the observed spin-echo spectrum for both nuclei arises from ferromagnetic islands (within an antiferromagnetic matrix) in the sample microscopically identical to the bulk metallic phase of the FMM manganites. Since for the rf power levels used, only ferromagnetic signals can be detected and since the spin-echo signal is observed down to 60 K, i.e., well below T_{CO}, a similar reasoning is valid for NSMO 0.5 as well.

The temperature dependence of the magnetization data suggests that, in NSMO 0.5, between T_C and T_{CO}, there is a strong competition between ferromagnetism, and antiferromagnetism leading to a CO state and charge localization at lower temperatures. Since we observe in NSMO 0.3 and 0.4 spectra just below T_C which resemble those of NSMO 0.5 above T_{CO}, we ascribe the complex spectra of NSMO 0.3 and 0.4 below T_C to a similar, though weaker, mechanism of carrier localization. As the temperature is further lowered, these resonances corresponding to localized charges disappear, leaving only a double-exchange spectrum of the metallic state.

In conclusion, ^{55}Mn -NMR was used as a local probe of magnetism and electronic structure that revealed the extent of complexity in the heterogeneity of the $Nd_{1-x}Sr_xMnO_3$ system. The comparative study of NSMO 0.1, 0.3, 0.4, and 0.5 by magnetic, resistive, and NMR measurements leads us to conclude that carrier localization takes place below T_C. The relaxation data confirm other observations of a Nd moment ordering around 15 K, leading to a DEX NMR spectrum more complex than that of LCMO.

ACKNOWLEDGMENTS

The authors would like to thank Jens Pommer, RWTH, Aachen, Germany for the magnetization data for NSMO (0.1, 0.2) and S. Angappane, IIT, Madras, for the resistivity and magnetization data on NSMO 0.5. One of us (M.P.) would like to thank the National Swiss Foundation for a grant. The work in the UK was supported by a grant from the EPSRC, UK.

*Present address: Department of Applied Chemistry, Royal Melbourne Institute of Technology (City Campus), Melbourne VIC-3001, Australia.

†Electronic address: rajan@acer.iitm.ernet.in

[1] A.J. Millis, Nature (London) **392**, 147 (1998).

[2] A. Moreo, S. Yunoki, and E. Dagotto, Science **283**, 2034 (1999).

[3] A. Lanzara, N.L. Saini, M. Brunelli, F. Natali, A. Bianconi, P.G. Radaelli, and S.-W. Cheong, Phys. Rev. Lett. **81**, 878 (1998).

[4] J.W. Lynn, R.W. Erwin, J.A. Borchers, Q. Huang, A. Santoro, J-L. Peng, and Z.Y. Li, Phys. Rev. Lett. **76**, 4046 (1996).

[5] E. Dagotto, S. Yunoki, and A. Moreo, Mater. Sci. Eng., B **63**, 65 (1999); G. Varelogiannis, Phys. Rev. Lett. **85**, 4172 (2000).

[6] G. Allodi, R. De Renzi, F. Licci, and M.W. Pieper, Phys. Rev. Lett. **81**, 4736 (1998).

[7] G. Papavassiliou, M. Fardis, M. Belesi, T.G. Maris, G. Kallias, M. Pissas, D. Niarchos, C. Dimitropoulos, and J. Dolinsek, Phys. Rev. Lett. **84**, 761 (2000).

[8] C. Xiong, Q. Li, H.L. Ju, S.N. Mao, L. Senapati, X.X. Xi, R.L. Green, and T. Venkatesan, Appl. Phys. Lett. **66**, 1427 (1995).

[9] V. Caignaert, A. Maignan, and B. Raveau, Solid State Commun. **95**, 357 (1995).

[10] N.H. Nam, R. Mathieu, P. Nordblad, N.V. Khiem, and N.X. Phuc, Phys. Rev. B **62**, 1027 (2000).

[11] A. Fernandez-Baca, P. Dai, H.Y. Hwang, C. Kloc, and S-W. Cheong, Phys. Rev. Lett. **80**, 4012 (1998).

[12] M. Pattabiraman, G. Rangarajan, K.-Y. Choi, P. Lemmens, G. Guentherodt, G. Balakrishnan, D.McK. Paul, and M.R. Lees, Pramana, J. Phys. **58**, 1013 (2002).

[13] G. Kaplan, M. Quijada, H.D. Drew, K.H. Ahn, A.J. Millis, R. Shreekala, R. Ramesh, M. Rajeshwari, and T. Venkatesan, Phys. Rev. Lett. **77**, 2081 (1996).

[14] Junghwan Park, M.S. Kim, J.-G. Park, I.P. Swainson, H.-C. Ri, H.J. Lee, K.H. Lee, K.H. Kim, T.W. Nohm, S.W. Cheong, and Changhe Lee, J. Korean Phys. Soc. **36**, 412 (2000).

[15] Kaiser, L.E. Stumpe, J.J. Rhyne, Y. Tokura, and H. Kuwahara, J. Appl. Phys. **85**, 5564 (1999).

[16] D.McK. Paul, Philos. Trans. R. Soc. London, Ser. A **356**, 1543 (1998).

[17] I. D. Weisman, L. J. Switzendruber, and L. H. Bennet, in *Techniques of Metal Research, VI*, edited by E. Passaglia (Wiley, New York, 1973), and references therein.

[18] H. Yoshizawa, R. Kajimoto, H. Kawano, J.A. Fernandez-Baca, Y. Tomioka, H. Kuwahara, and Y. Tokura, Mater. Sci. Eng., B **63**, 125 (1999).

[19] Superparamagnetic behavior has been detected from Mossbauer studies on various manganites. For example, see: Vladimir Chechersky, Amar Nath, Claude Michel, Maryvonne Hervieu, Kartik Ghosh, and Richard L. Greene, Phys. Rev. B **62**, 5316 (2000).

[20] H. Kuwahara, Y. Tomioka, A. Asamitsu, Y. Moritomo, and Y. Tokura, Science **270**, 961 (1995).

[21] Satoshi Awaji, Kazuo Watanabe, Manabu Fujiwara, Yosuke Watanabe, and Norio Kobayashi, Physica B **284-288**, 1682 (2000).

[22] G. Matsumoto, J. Phys. Soc. Jpn. **29**, 615 (1970).

[23] A. J. Freeman and R. E. Watson, in *Magnetism, IIA*, edited by G. T. Rado and H. Shul (Academic Press, New York, 1966).

[24] T. Kubo, H. Yasuoka, and A. Hirai, J. Phys. Soc. Jpn. **21**, 812 (1966).

[25] T. Kubo, A. Hirai, and H. Abe, J. Phys. Soc. Jpn. **26**, 1094 (1969).

[26] L.K. Leung and A.H. Morrish, Phys. Rev. B **15**, 2485 (1977).

[27] Joonghoe Dho, Ilryong Kim, and Soonchil Lee, Phys. Rev. B **60**, 14 545 (1999).

[28] C. Kapusta, P.C. Reidi, W. Kocemba, G.J. Tomka, M.R. Ibarra, J.M. De Teresa, M. Viret, and J.M.D. Coey, J. Phys.: Condens. Matter **11**, 4079 (1999).

[29] G. Papavassiliou, M. Fardis, M. Belesi, I. Panagiotopoulos, G. Kallias, D. Niarchos, C. Dimitropoulos, and J. Dolinsek, Phys. Rev. B **59**, 6390 (1999).

[30] T.Y. Koo, V. Kiruyukhin, P.A. Sharma, J.P. Hill, and S-W. Cheong, Phys. Rev. B **64**, 220405 (2001).

[31] E. Gordon, R.A. Fischer, Y.X. Jia, N.E. Philips, S.F. Reklis, D.A. Wright, and A. Zettl, Phys. Rev. B **59**, 127 (1999).

[32] H.H. Hamdeh, J.C. Ho, S.A. Oliver, J.G. Lin, S.Y. Lin, P.C. Kuo, and C.Y. Huang, J. Magn. Magn. Mater. **232**, 175 (2001).